

Multi-reference Poly-conformational Computational Methods for De-novo Design, Optimization, and Repositioning of Pharmaceutical Compounds.

Vadim Alexandrov

Liquid Algo LLC

Alexander Kirpich

Georgia State University

Yuriy Gankin (✉ yuriy.gankin@quantori.com)

Quantori LLC

Research Article

Keywords: COVID-19, conformers, multi-reference, poly-conformational, in silico, ligand-based, structure-based, SARS-COV-2, fingerprints, cheminformatics, similarity, virtual library, computational framework

Posted Date: February 4th, 2021

DOI: <https://doi.org/10.21203/rs.3.rs-153954/v1>

License:   This work is licensed under a Creative Commons Attribution 4.0 International License.

[Read Full License](#)

1 **Multi-reference poly-conformational computational methods for de-novo**
2 **design, optimization, and repositioning of pharmaceutical compounds.**

3

4 **Vadim Alexandrov¹, Alexander Kirpich² and Yuriy Gankin*³**

5

6 **1 Liquid Algo LLC, 85 Thistle Lane, Hopewell Junction, NY 12533, United States of America**

7 **2 School of Public Health, Georgia State University, Atlanta, Georgia, United States, Atlanta,**
8 **GA, United States of America**

9 **3 Quantori LLC, 625 Mass Ave, Cambridge, MA 02139, United States of America**

10 *** Corresponding author**

11 **E-mail: yuriy.gankin@quantori.com**

12

13

14

15

16

17

18

19

20 **ABSTRACT**

21 The COVID-19 epidemic, SARS-CoV-2, that began in December of 2019 has drastically altered
22 the aspects of daily life across the global society. Time-effective treatment of those infected has
23 since become a major goal with multiple treatment strategies having been designed to prevent the
24 progression of the disease into severe pneumonia. To date, no drug has been found to be 100%
25 effective against SARS-COV-2, possibly because each candidate drug was targeting only one
26 particular mechanism of action (MoA). Neither proposed up-to-date anti-SARS-COV-2 vaccine
27 are 100% effective. To contribute to the process of finding a more robust small-molecule solution,
28 utilizing several anti-SARS-COV-2 MoAs, a novel framework is presented; where the in silico
29 generated set of virtual library compounds is compared to six known reference drugs: Chloroquine,
30 Favipiravir, Remdesivir, JQ1, Apicidine, and Haloperidol which have been already used for
31 SARS-CoV-2 treatment. The aims were: a) to present a universal search framework for potential
32 candidate compounds based on the comparison of multiple similarities between compounds’
33 conformers and b) to identify candidate compounds that are simultaneously “close” to each of the
34 six known reference compounds that counteract SARS-CoV-2 via different mechanisms of action.

35

36 **KEYWORDS**

37 COVID-19, conformers, multi-reference, poly-conformational, in silico, ligand-based, structure-
38 based, SARS-COV-2, fingerprints, cheminformatics, similarity, virtual library, computational
39 framework

40

41

42 INTRODUCTION

43 **The necessity of the transparent algorithm.** The novel coronavirus SARS-CoV-2 was
44 introduced into the human population in the Chinese city of Wuhan in the Province of Hubei in
45 December of 2019 ¹⁻⁴. Since then the epidemic of SARS-CoV-2 has rapidly spread Worldwide.
46 The World Health Organization (WHO) has officially declared the SARS-CoV-2 pandemic in
47 March 2020 just three months after its emergence ⁵. The novel coronavirus received an official
48 name SARS-CoV-2 and the virus pandemic was called COVID-19 ⁶. As of November 2020, there
49 has been no virus-specific treatment for SARS-CoV-2 ⁷ but multiple drugs have been proposed,
50 such as remdesivir ⁸, talampicillin, lurasidone, rubitecan, loprazolam ^{9,10}, chloroquine, and
51 hydroxychloroquine ^{9,10}, atazanavir ¹¹, azithromycin, quercetin, chloroquine, rapamycin, and
52 doxycycline ¹². The formal evaluation and comparison of drugs can be performed by studying the
53 compound properties by treating patients and performing clinical trials ^{7-10,12} or by studying the
54 properties of the corresponding compounds in silico ^{9,11}. The computational methods are
55 preliminary and exploratory, but are less invasive than clinical trials and allow the simultaneous
56 study of large quantities of potential compounds. Since none of the proposed small molecules were
57 found to be 100%-effective, we present a new computational method that combines the best
58 features from the earlier individually imperfect small-molecule treatments.

59 **Conformers as independent molecular entities.** In real life, most compound molecules exist in
60 multiple conformations (shapes) based on the surrounding environmental conditions. In particular,
61 each 3D shape of a molecule dictates its biological activity and enables the molecule to fit into the
62 binding pockets of proteins. Often, distinctly different chemical compounds that have similar
63 shapes (and similar charge distributions along the molecular surface) can bind as long as the
64 ligand's partial charges are positioned in the binding pocket the same way (i.e., form the same

65 hydrogen bonds). Therefore, it is beneficial to compare the shapes and surface distribution charges
66 for target query and reference compounds on a conformer-by-conformer basis. If one of the
67 conformers of the query molecule matches one of the conformers (especially bound-to-target) of
68 the reference molecule, then there is a chance that the reference compound will also exhibit similar
69 binding properties to the same target.

70 **Alignment-free 3D-similarity scoring.** OpenEye Scientific Software Inc. pioneered an algorithm
71 and the corresponding tool ROCS¹³ for comparing shapes of molecules by overlaying and
72 measuring their molecular structures in silico and comparing differences between a query and
73 target molecule. ROCS identifies potentially active compounds by comparing their shapes.
74 Moreover, the ROCS tool is competitive and often superior to structure-based approaches in virtual
75 screening^{14,15} both in terms of overall performance and consistency¹⁶. As a result novel, molecular
76 scaffolds have been identified by using ROCS against various targets which have been considered
77 very difficult to address computationally¹⁷.

78 **Challenges with overlaying.** The process of molecular shapes overlaying remains
79 computationally intensive and often is a bottleneck in the search process for similar molecules.
80 This remains despite the recent so-called PAPER implementation of ROCS on GPU¹⁸ and the
81 development of FastROCS¹⁹ for large (>1B) compound libraries. Recently, alternative methods
82 for overlaying have been introduced as a substitute for the ROCS approach. The alternative
83 overlaying is performed by comparing shape-based descriptors (a.k.a conformer-level 3D
84 fingerprints). An example of such an approach is ElectroShape implemented in the ODDT package
85²⁰ and is based on the algorithm that incorporates shape, chirality, and electrostatics^{21,22}, and
86 represents each conformer via a fixed-length vector of real-valued numbers. Similarly the E3FP
87 package²³ also utilizes an alignment-invariant 3D representation of molecular conformers as a

88 fixed-length binary vector for each conformer. These fingerprint-based approaches allow to
89 calculate the similarity between two molecular shapes either as a Tanimoto distance (for binary
90 fingerprints) or Euclidean distance (for real-valued fingerprints) computations. Such computations
91 are orders of magnitude faster in comparison to alternative methods that require the actual
92 alignment of the two compared conformers. Even though the calculation of a shape-based
93 fingerprint for each conformer can be a rather computationally involved procedure, as soon as all
94 conformers for the virtual library are fingerprinted and stored in a database, the similarity search
95 for the query molecule in such a database is computationally quick. Therefore the computationally
96 efficient method proposed here is expected to be very useful for finding candidate drugs for multi-
97 target disease indications, ligand-based drug design, and drug repurposing applications.

98

99 **METHODS**

100 **Conformer-by-conformer comparison.** The proposed computational algorithm extends the
101 currently available methods²⁰⁻²³ and introduces additional search flexibility via the use of the
102 compound conformers. The proposal is to compare multiple possible shapes, adopted via varying
103 environmental conditions, of the same molecule (i.e., conformers) rather than just a single shape
104 that was used before. In particular, the suggested approach is based on the matching of ligand-
105 ligand fingerprints and goes beyond the known docking methods that utilize the simulated physical
106 binding of a ligand to the target. The supporting theory behind the method is based on the decision
107 to treat conformers, which might have different binding characteristics and properties, as
108 independent entities. In such an approach each conformer has the corresponding independent
109 alignment-free 3D-similarity scoring using the known multi-references. All conformers were
110 generated using the ETKDG algorithm implemented in RDkit²⁴. Benchmarking studies have

111 found ETKDG to be the best-performing freely available conformer generator up-to-date ^{25,26}
112 providing diverse and chemically-meaningful conformers reproducing crystal conformations.

113 The authors have called the approach MultiRef3D to emphasize that it is a fast, alignment-free
114 multi-objective optimization protocol that maximizes the 3D overlap of a query molecule's
115 conformational ensemble with conformational ensembles of multiple reference ligands.

116 **Efficiency and a conformer scoring.** In the algorithm, each conformation is treated as an
117 independent entity and is characterized by a vector of features (fingerprint) which describes its 3D
118 shape along with the distribution of electrostatic charge across its molecular surface. The
119 generated fingerprints reflect both 3D and surface charge (both denoted further as 3D+charge) for
120 each query molecule conformer as well as for all conformers of the reference compound. In this
121 case, each conformer is coded within the algorithm by a single fingerprint represented as a vector
122 of numbers which ensures computational efficiency. Those fingerprints for each of the query
123 molecule conformers are individually scored by Euclidean distance as a similarity measure
124 concerning each conformer of the reference compound. The Euclidean distance can be viewed as
125 an extension of the Tanimoto similarity measure for non-binary fingerprints. The fingerprinting of
126 individual conformers for alignment-free comparisons became popular in the past couple of years
127 ^{23,27-29} so the proposed method is built on those.

128 **Objective Function Optimization.** The sum of the conformer-to-conformer similarity scores
129 between the query and a reference compound are compared via an objective similarity function W_c
130 for each reference compound c . The goal is to maximize the sum of those individual objective
131 similarity functions across all reference compounds of interest $c=1,2,\dots,C$ where c is a summation
132 index for the desired set of reference compounds:

133
$$W_{All} = \sum_{c=1}^C W_c = \sum_{c=1}^C \sum_{q=1}^Q \sum_{r=1}^R S_{q,r}^{(c)} \quad (1)$$

134 In formula (1) the summand $S_{q,r}^{(c)}$ is the similarity (overlap) of the query conformer q ($q=1,2,\dots,Q$)
 135 with the conformer r ($r=1,2,\dots,R$) for each reference compound c ($c=1,2,\dots,C$). For the real-valued
 136 fingerprints, the similarity summand between the pair of conformers of interest indexed by query
 137 index q and reference index r for compound c is calculated as:

138
$$S_{q,r}^{(c)} = 1 - (1/N) \sqrt{\sum_{n=1}^N (x_{q,n}^{(c)} - x_{r,n}^{(c)})^2} \quad (2)$$

139 where $x_{q,n}^{(c)}$ and $x_{r,n}^{(c)}$ are the corresponding normalized fingerprint vector coordinates for
 140 $n=1,2,\dots,N$. The length (the number of coordinates) of the fingerprint N is determined based on
 141 the problem-specific target-ligand interaction characteristics. Since the fingerprint coordinates $x_{q,n}^{(c)}$
 142 and $x_{r,n}^{(c)}$ are normalized (i.e. have values between 0 and 1 for each coordinate n) the resulting
 143 overlap $S_{q,r}^{(c)}$ is maximized with the value equal to 1 when the fingerprints of both conformers are
 144 identical and can take the smallest value equal to 0 when all the fingerprint coordinates have a
 145 difference equal to 1 i.e. as different as possible at the normalized scale.

146 When the objective is to identify a novel compound for just a single active conformation ($r=1$) of
 147 one ($c=1$) reference compound (e.g. a reference ligand co-crystallized with one particular target)
 148 then all conformers for the query molecule are scored against only one active reference conformer.
 149 However, in the case when multiple reference compounds are bound to the same target (or sets of
 150 reference compounds bound to multiple targets), the total objective function comes into play. It is
 151 important to point out that the proposed method is not limited to the structure-based design
 152 situations: when several reference compounds are found to be active in a functional assay (and
 153 either the target(s) is unknown or the crystal structure of the target is not available) - the formula

154 works just as well (as long as the ligand structure is known). The method becomes especially
155 handy, when there is a great diversity among active reference compounds, whether the target
156 structural information is known or not – the objective function will extract and sum up the
157 similarities for all of the relevant parts of the fingerprinted conformer representations responsible
158 for the observed activity.

159 The query compound can be evaluated against multiple reference compounds on a conformer-by-
160 conformer basis. In such a case, the corresponding similarity scores are summed and constitute
161 the multi-reference conformer-level objective function to maximize. This can be readily used in a
162 typical ligand-based design setting. However, instead of just searching for a shape analog of one
163 of the conformers of a reference compound, in the case of multiple references, the algorithm
164 performs a search for such a compound in the virtual library whose conformers have overlapped
165 with conformers of each of those reference compounds. The latter will increase the chances that
166 the selected virtual compound binds the same way to the corresponding targets of each of the
167 references (i.e. the selected compound is capable of forming conformations that resemble active
168 conformations responsible for the Mechanism-of-Action (MoA) of each of the references).

169 **Selection of the reference compounds and conformers.** In total six diverse compounds from
170 ClinicalTrials.gov³⁰ that are currently undergoing clinical trials for SARS-CoV-2 treatment have
171 been selected as reference compounds. These compounds are diverse in the sense that their
172 chemical structures differ substantially (i.e. Tanimoto distance < 0.7) from each other, and they all
173 have specificity for different targets, i.e. different Mechanism-of-Action (MoA). Three of these
174 compounds (Chloroquine³¹, Remdesivir³², and Favipiravir³³) have recently demonstrated
175 significant efficacy against SARS-COV-2, whereas JQ1, Apicidin, and Haloperidol are already
176 marketed compounds well-known for their efficacy against other disease indications. One hundred

177 conformers for each of the reference molecules were generated at the MMFF94 level of theory ³⁴
178 and each conformer was ODDT-fingerprinted ²⁰ and saved in the MongoDB database ³⁵. The
179 ODDT implementation ²⁰ of ElectroShape fingerprints ²² has been selected to demonstrate the
180 proposed approach because these fingerprints are considered to be state-of-the-art in ligand-based
181 virtual screening experiments ^{36,37}, and they are not limited to binary values.

182 Sometimes (e.g. at the beginning of a drug discovery program) a good virtual library might not
183 exist yet and fingerprinting the entire ZINC15 database ³⁸ or Enamine REAL database ³⁹ can be
184 computationally expensive (it may take several months to ODDT-fingerprint either of these
185 databases on a single CPU). Therefore in this work, two simplified approaches have been used to
186 illustrate the method. The first one is a focused virtual library approach that screened “only”
187 100,000 compounds from focused Enamine libraries, such as “anti-viral-like”. The second one is
188 an optimization based on a focused reference compound which is already known to be effective
189 for the target goals (e.g., start the optimization from a SARS-COV-2 reference compound, such as
190 chloroquine).

191 **Focused virtual library screening.** For the first approach, the virtual library (query compounds)
192 consisted of Enamine focused virtual sets (antiviral and other specialized libraries) from the
193 Enamine REAL database ³⁹. Molecules from this virtual library were simultaneously evaluated
194 against several antiviral reference drugs with different mechanisms of action (e.g. in the SARS-
195 COV-2 case the three major currently pursued MoA-s are: ACE2 binding, Mpro and RdRP
196 inhibition). A query molecule for which some of the conformers are similar in shape with
197 conformers for all the reference drugs would receive a higher score. In this approach, multiple
198 virtual compounds can be identified to have a good conformer overlap with the reference drugs.

199 The proposed in silico optimization algorithm from a focused reference compound (i.e.
200 chloroquine) is as follows:

- 201 1. Start in-silico synthesis (transformation) of any active compound in the training set by
202 applying chemical transformation rules from chemical reaction databases that ensure
203 tractability ("synthesizability") of each new "in-silico" compound obtained using these
204 rules (i.e each rule is a documented feasible transformation of a particular compound class
205 or compound substructure).
- 206 2. After each transformation, fingerprint all conformers from the obtained novel in-silico
207 compound and calculate the total overlap score with the reference conformers.
- 208 3. Based on the value of the total overlap score:
 - 209 a. reject novel compounds with low scores.
 - 210 b. keep transforming the top N (e.g. $N = 10$) highest scored compounds.
- 211 4. Stop the optimization procedure when the top score at the current iteration is no longer
212 higher than the top score in the previous iteration.

213

214 **RESULTS**

215 **Focused virtual library screening for SARS-CoV-2 compounds.** For the first approach, scoring
216 has been performed for the six compounds that are used for SARS-CoV-2 treatment i.e.
217 Chloroquine, Remdesivir, Favipiravir, JQ1, Apicidine, and Haloperidol. The algorithm visual
218 summary is displayed in Fig. 1 for the W_{All} objective function. Table 1 summarizes the direct
219 application results of the focused antiviral Enamine virtual sub-library screening. The first two

220 columns of Table 1 contain query compounds from the Enamine REAL database ³⁹ and their
 221 computed overlap scores. The rows are sorted according to the total sum overlap score displayed
 222 in the second column. The first two compared virtual compounds (Virt-cpd-001 through Virt-
 223 cpd-004) have the maximum sum of scores without “gaps”, i.e. none of the compounds have a
 224 score equal to zero indicating no overlap. This is different from compound Virt-cpd-014 whose
 225 conformers had no overlap with any of the conformers of Chloroquine, Remdesivir, and JQ1 but
 226 had a “good” overlap (in terms of the score) with conformers of Favipiravir, Apicidin, and
 227 Haloperidol.

228 **Table 1.** The query compounds from a virtual library (the first column) are sorted by their total
 229 overlap score W_{All} (the second column). The values in the other columns correspond to the sums
 230 of the overlap scores of the conformers for the corresponding reference compounds.

231

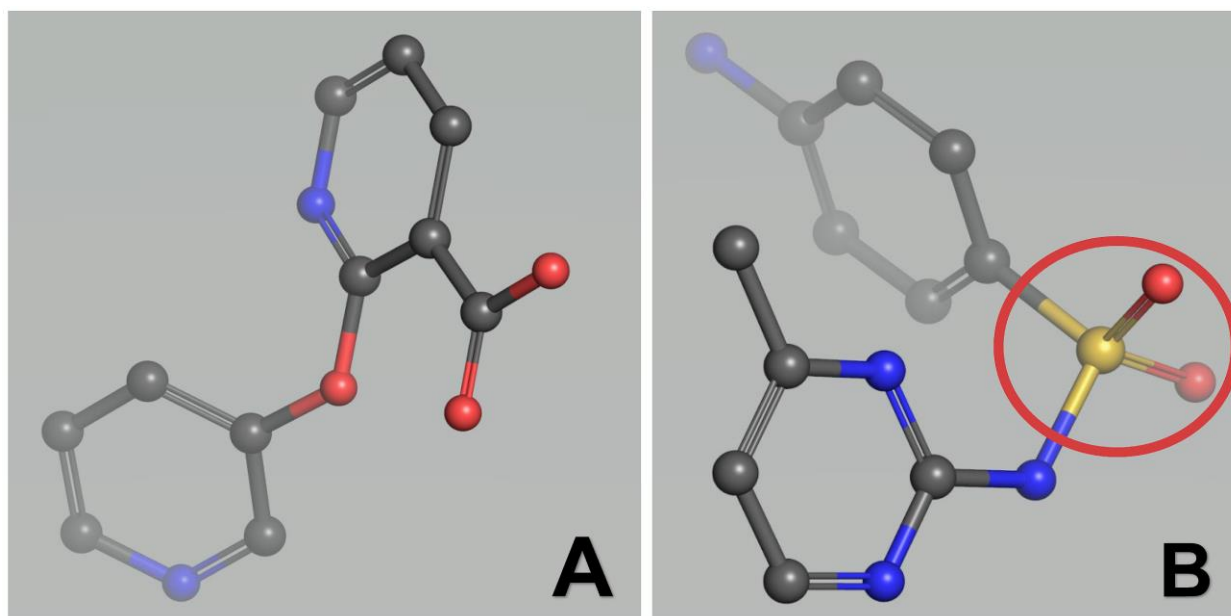
Virtual Compound	W_{All}	Choloroquine	Remdesivir	Favipiravir	JQ1	Apicidin	Haloperidol
Virt-cpd-001	354.37	58.25	58.30	59.14	59.38	59.34	59.94
Virt-cpd-002	283.28	48.73	24.64	36.07	50.53	61.31	62
Virt-cpd-003	282.95	48.1	25.8	37.26	49.85	60.61	61.34
Virt-cpd-004	269.63	37.87	23.46	46.09	39.12	61.06	62.03
Virt-cpd-005	241.03	29.27	0	59.51	29.87	60.58	61.78
Virt-cpd-006	209.92	34.42	34.61	34.93	34.94	35.35	35.67
Virt-cpd-007	182.34	21.04	22.94	38.17	21.41	38.08	40.7
Virt-cpd-008	173.60	45.31	20.82	0	46.62	21	39.85
Virt-cpd-009	172.77	32.23	32.1	0	45.28	29.81	33.36
Virt-cpd-010	168.55	32.29	11.72	16.28	33.49	31.1	43.67
Virt-cpd-011	165.05	0	18.2	31.89	20.03	42.59	52.34
Virt-cpd-012	155.42	39.85	0	11.76	34.63	34.39	34.8

Virt-cpd-013	152.10	39.57	0	0	39.44	26.97	46.12
--------------	--------	-------	---	---	-------	-------	-------

232

233 When interpreting the results displayed in Table 1, the individual scores for each reference
234 compound should be taken into account along with the total score. For example, while compounds
235 Virt-cpd-012 and Virt-cpd-013 have very similar scores, conformers for Virt-cpd-014 have no
236 overlap with conformers of Remdesivir or Favipiravir, whereas conformers of Virt-cpd-012 have
237 no overlap only with conformers of Remdesivir. Since the objective is to find a compound whose
238 conformers have overlap with conformers for all of the reference compounds that have been
239 selected for the algorithm it is concluded that Virt-cpd-013 is substantially worse than Virt-cpd-
240 012. The other illustrative example is a total score comparison of Virt-cpd-005 vs Virt-cpd-006.
241 Even though the score for Virt-cpd-005 is higher than that for Virt-cpd-006, none of the conformers
242 of Virt-cpd-005 have any overlap with conformers of Remdesivir. The total score of Virt-cpd-005
243 is higher because the overlap of its conformers with those of Apicidin and Haloperidol is a lot
244 higher than the corresponding overlaps for Virt-cpd-006. Therefore based on Table 1. the
245 compounds Virt-cpd-006, Virt-cpd-007, Virt-cpd-008, Virt-cpd-011, Virt-cpd-012, and Virt-cpd-
246 013 are not recommended for the followup in-vivo tests since those compounds have no overlap
247 with any of the conformers for one of the reference compounds. A filter can be imposed for those
248 virtual compounds that have zero overlap with at least one of the references since the *multi-*
249 *objective* goal is to identify those virtual compounds that have the potential to exhibit *all* aspects
250 of the therapeutic intervention for each of the reference compounds. Therefore the compounds
251 with at least one such zero overlap are not recommended for the follow-up *in-vivo* testing
252 experiments.

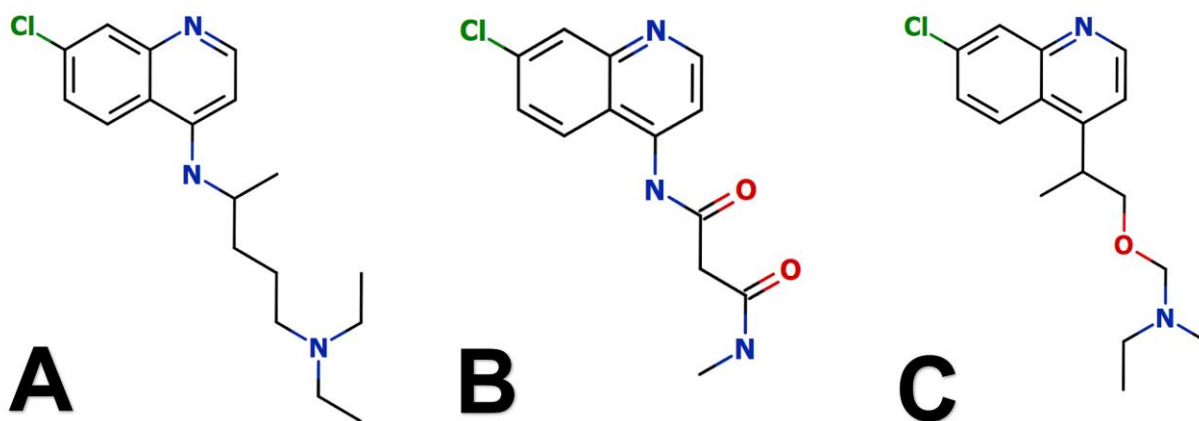
253 For the visual illustration of the algorithm results two compounds with the highest scores from
254 Table 1. have been presented in Fig. 1. It is with noting that these compounds form very flexible
255 molecules due to their either sulphonyl or ether bridge around which the ring substructures can
256 rotate, which ensures the ability of those molecules to accommodate different targets.



257
258 Fig 1. The compounds presented in panels **A** and **B** from the antiviral Enamine virtual sub-library
259 collection that were found to maximize conformer overlap scores with the six reference
260 compounds. In addition to that sulphonyl bridge in panel **B** (circled in red) is a signature of the
261 classic antiviral compounds (e.g. well-known drug sulfapyridine), as well as the ether bond. The
262 bridge allows for 3D flexibility for the molecule to change conformation and bind to multiple
263 targets.

264 **In-silico optimization of a specific drug (chloroquine).** For the second approach chloroquine
265 drug has been selected for the illustration of the optimization from a focused single reference
266 compound. The selected chloroquine has been used as a starting point for the algorithm. For this
267 starting point, it has been discovered that the in-silico modification/optimization procedure quickly

268 converges to a series of novel compounds with high scores exceeding the highest score in the
269 original starting compound. The visual summary of the optimization results based on NOVA⁴⁰ in-
270 silico synthesis and selection for higher overall overlap are presented in Fig 2.



272 **Fig 2.** The original chloroquine is presented in panel **A**, while the chloroquine analogs optimized
273 in the modify-score-select algorithm are presented in panels **B** and **C**.

274

275 In Fig. 2 the compounds in panels B and C can be visually compared to the original chloroquine
276 structure in panel A. One can see that the two joined rings, the structural signature of chloroquine,
277 remained in the final optimized structures untouched by the optimization process (modifications
278 to that moiety would decrease the score and thus were rejected for the next iteration). This
279 approach can be viewed as building and scoring virtual library on-the-fly where the seed is chosen
280 to be one of the reference compounds. This can save a lot of compound generation scoring effort
281 (in contrast to scoring a comprehensive 140-billion conformation) library but might not hop too
282 far from the chemical neighborhood of the seed compound (the latter is not a drawback but rather
283 a desired feature during lead optimization effort around e.g. a patented chemotype or well-
284 researched chemical space in an already advanced lead optimization program).

285 **DISCUSSION**

286 **Application for drug-repurposing.** Depending on what is known about the indication or
287 marketed drug of interest (targets, MoAs, other existing drugs for the same indication) the
288 proposed methods (or a combination thereof) can be used to find other non-obvious molecules
289 whose shape and the surface electrostatic charge is similar to that of the marketed drug. The
290 methods can also be used to search for the cumulative similarity to conformers of the multiple
291 drugs used to treat this disease indication.

292 **Special note on the use of non-lowest energy conformations and SARS-CoV-2.** Unlike what
293 the majority of computational methods had assumed a couple of decades or so ago (e.g. in the
294 CoMFA method ⁴¹), recent research indicates that the bioactive conformation is not necessarily
295 the lowest-energy conformation in the absence of the receptor ⁴²⁻⁴⁴. In particular, as long as an
296 increase in energy for less favorable conformation is compensated by its binding to the target, i.e.
297 the total ligand-target energy is lower than the sum of the energies for the non-bound target and
298 ligand, the bound state is favored. The proposed method emphasizes and relies on this ligand's
299 ability to use its higher energy conformations depending on the target it attempts to bind.
300 Moreover, in the proposed method multiple conformers of the query ligand have been compared
301 with conformers from *multiple* reference compounds whose therapeutic effect of interest is
302 achieved via different mechanisms of bindings to different targets, e.g. by inhibiting Main protease
303 (Mpro) ⁴⁵ and RNA-dependent RNA polymerase (RdRP) ⁴⁶, while at the same time elevating pH
304 in lysosomes to arrest the intracellular proliferation of SARS-CoV-2 ^{47,48}. An "ideal drug" would
305 contain conformers that resemble (some) conformers of all of the reference drugs, thus by
306 increasing chances that the drug inhibits SARS-CoV-2 via multi-MoA routes and is more effective
307 than each individual reference drug.

308 **Note on applications for structure-based designs.** When the crystal structure of the target protein
309 is known and the reference ligand is co-crystallized in its active conformation (structure-based
310 design), we can use this information about the reference compound and evaluate the query
311 molecules against only one, the active (co-crystallized) reference ligand conformation ($r = r_{active}$)
312 in formulas (1) and (2). Confirmation by direct docking for the fingerprint-matched queries can be
313 used to confirm the match.

314 Our methodology emphasizes pursuit of candidate compounds that achieve therapeutic effect (e.g.
315 stops SARS-CoV-2 proliferation) by multiple MoA routes. A successful candidate compound
316 would contain conformers targeting M-protease, RdRP and endosome virus trafficking MoAs all
317 at the same time by increasing chances that the compound would protect against SARS-CoV-2
318 much more effectively. Naturally, all successful candidates would need to be further screened and
319 filtered for proper ADME-Tox and other drug-likeness properties. Binding to anti-targets, e.g.
320 hERG, can be explicitly incorporated to this methodology by adding the corresponding terms
321 (similarities to known hERG-binding ligands) to the overlap sum with a negative sign. Even
322 though many computational methods exist to evaluate hERG in particular as well as other common
323 tox liabilities, when an anti-target is very specific and less commonly known as “pure tox target”
324 (e.g. undesired binding to D2 receptor for many modern CNS drugs), the explicit inclusion of
325 similarity score to such anti-target with a negative sign can greatly streamline the overall drug
326 optimization process.

327 **CONCLUSION**

328 We have demonstrated the usefulness of the multi-reference optimization approach in various in-
329 silico drug discovery settings and illustrated its application for de-novo ligand-based design,
330 optimization, and repositioning of pharmaceutical compounds. The results allow the representation

331 of each molecule as an ensemble of flexible conformers that would choose the best possible
332 conformation for each presented target-binding opportunity that can be applied in multiple settings.
333 Application of this approach to SARS-CoV-2 produced several antiviral drug candidates that are
334 designed to protect against SARS-CoV-2 by multiple mechanisms simultaneously.

335

336 **LIST OF ABBREVIATIONS**

337 ADME-Tox - Absorption, Distribution, Metabolism, Excretion and Toxicity

338 GPU - Graphics processing unit

339 CNS - Central nervous system

340 CoMFA - Comparative molecular field analysis

341 COVID-19 - Coronavirus Disease of 2019

342 CPU - Central processing unit

343 hERG - Human Ether-a-go-go-related Gene

344 MoA(s) - Mechanism of Action(s)

345 ODDT - Open Drug Discovery Toolkit

346 RNA - Ribonucleic acid

347 ROCS - Rapid overlay of chemical structures

348 SARS-CoV-2 - Severe acute respiratory syndrome coronavirus 2

349 WHO - World Health Organization

350 **DECLARATIONS**

351 **Availability of data and materials**

352 Code that has been used for analysis and for manuscript preparation can be found at Quantori
353 public GitHub repository online ⁴⁹. Data (ligand structures) from REAL focused libraries can be
354 downloaded from the Enamine Ltd. website ⁵⁰.

355 **Competing interests**

356 The proposed method has been submitted for a patent. The patent application number is 63061790
357 at the United States Patent and Trademark Office and as of October 17, 2020, the patent is pending.
358 The patent can be a source of financial income for authors Vadim Alexandrov (VA) and Yuriy
359 Gankin (YG).

360

361 **Funding**

362 The author Vadim Alexandrov (VA), a founder of a consulting company Liquid Algo LLC in
363 Hopewell Junction, New York, United States received no compensation for this work. The author
364 Yuriy Gankin (YG) is employed by the commercial company Quantori in Cambridge,
365 Massachusetts, United States. Alexander Kirpich (AK) is employed at the School of Public Health
366 at a non-profit institution Georgia State University. Quantori provided support in the form of salary
367 and relevant publication and patent fees for YG. YG received no compensation for this work. AK
368 received no funding or any other financial support for this project.

369

370 **Authors' contributions**

371 Vadim Alexandrov (VA), Alexander Kirpich (AK), and Yuriy Gankin (YG) are the authors of the
372 manuscript. VA and YG proposed the manuscript idea, obtained the data, implemented routine
373 coding operations, and wrote the preliminary version of the manuscript. AK performed an
374 additional literature review and wrote the final version of the manuscript. YG also provided the
375 overall guidance for the project and participated in the manuscript preparation.

376 **Acknowledgments**

377 The authors would like to acknowledge Nika Tsutskiridze and Daviti Khatchilava for their
378 assistance in extracting information from clinical trials and peer reviewed literature. The authors
379 also want to acknowledge Alexander Proutsky and John Reynders for their suggestions and
380 comments during the manuscript preparation.

381 **Authors' information**

382 VA holds a Ph.D. in Computational Chemistry from The University of Arizona and a Ph.D. in
383 BioInformatics from Yale University. He has over 20 years of experience in computer-aided drug
384 design and pioneered hit generation and lead optimization paradigm in high-throughput in-vivo
385 phenotypic drug discovery.

386 AK is a biostatistician and an assistant professor in the Department of Population Health Sciences
387 at the School of Public Health at Georgia State University. AK holds a Ph.D. in biostatistics from
388 the University of Florida and has expertise in infectious disease statistical modeling (cholera,
389 dengue, HIV, anthrax, and others), epidemiology, and bioinformatics. The interests and goals of
390 AK are broad and target application of statistical methods to public health and biomedical research

391 questions and policies and to address statistical challenges, such as missing data, asymptomatic
392 infections, underreporting, and noise during data acquisition.

393 YG serves as Chief Scientific Officer at Quantori, a developer of intelligent IT and data science
394 solutions for life science, pharma, and healthcare organizations. Yuriy's expertise is in analytical
395 chemistry, data science, and chem- and bioinformatics. He holds a Ph.D. in Analytical Chemistry
396 from Tufts University and an MBA from the Massachusetts Institute of Technology Sloan School
397 of Management.

398

399

400

401

402

403

404

405

406

407

408

409

410

411

412

413 **REFERENCES**

414

415 1. Zhu, N. *et al.* A Novel Coronavirus from Patients with Pneumonia in China, 2019. *N. Engl.*
416 *J. Med.* **382**, 727–733 (2020).

417 2. Lu, H., Stratton, C. W. & Tang, Y.-W. Outbreak of pneumonia of unknown etiology in
418 Wuhan, China: The mystery and the miracle. *J. Med. Virol.* **92**, 401–402 (2020).

419 3. Huang, C. *et al.* Clinical features of patients infected with 2019 novel coronavirus in
420 Wuhan, China. *The Lancet* vol. 395 497–506 (2020).

421 4. Chen, N. *et al.* Epidemiological and clinical characteristics of 99 cases of 2019 novel
422 coronavirus pneumonia in Wuhan, China: a descriptive study. *The Lancet* vol. 395 507–513
423 (2020).

424 5. WHO Director-General’s opening remarks at the media briefing on COVID-19 - 11 March
425 2020. [https://www.who.int/dg/speeches/detail/who-director-general-s-opening-remarks-at-](https://www.who.int/dg/speeches/detail/who-director-general-s-opening-remarks-at-the-media-briefing-on-COVID-19---11-march-2020)
426 [the-media-briefing-on-COVID-19---11-march-2020.](https://www.who.int/dg/speeches/detail/who-director-general-s-opening-remarks-at-the-media-briefing-on-COVID-19---11-march-2020)

427 6. Naming the coronavirus disease (COVID-19) and the virus that causes it.
428 [https://www.who.int/emergencies/diseases/novel-coronavirus-2019/technical-](https://www.who.int/emergencies/diseases/novel-coronavirus-2019/technical-guidance/naming-the-coronavirus-disease-(covid-2019)-and-the-virus-that-causes-it)
429 [guidance/naming-the-coronavirus-disease-\(covid-2019\)-and-the-virus-that-causes-it.](https://www.who.int/emergencies/diseases/novel-coronavirus-2019/technical-guidance/naming-the-coronavirus-disease-(covid-2019)-and-the-virus-that-causes-it)

430 7. Cascella, M., Rajnik, M., Cuomo, A., Dulebohn, S. C. & Di Napoli, R. Features,
431 Evaluation, and Treatment of Coronavirus (COVID-19). in *StatPearls [Internet]* (StatPearls
432 Publishing, 2020).

433 8. Sanders, J. M., Monogue, M. L., Jodlowski, T. Z. & Cutrell, J. B. Pharmacologic
434 Treatments for Coronavirus Disease 2019 (COVID-19): A Review. *JAMA* (2020)
435 doi:10.1001/jama.2020.6019.

436 9. Elmezayen, A. D., Al-Obaidi, A., Şahin, A. T. & Yelekçi, K. Drug repurposing for

- 437 coronavirus (COVID-19): screening of known drugs against coronavirus 3CL hydrolase and
438 protease enzymes. *J. Biomol. Struct. Dyn.* 1–13 (2020).
- 439 10. Zhang, W. *et al.* The use of anti-inflammatory drugs in the treatment of people with severe
440 coronavirus disease 2019 (COVID-19): The experience of clinical immunologists from
441 China. *Clin. Immunol.* 108393 (2020).
- 442 11. Beck, B. R., Shin, B., Choi, Y., Park, S. & Kang, K. Predicting commercially available
443 antiviral drugs that may act on the novel coronavirus (SARS-CoV-2) through a drug-target
444 interaction deep learning model. *Comput. Struct. Biotechnol. J.* **18**, 784–790 (2020).
- 445 12. Sargiacomo, C., Sotgia, F. & Lisanti, M. P. COVID-19 and chronological aging: senolytics
446 and other anti-aging drugs for the treatment or prevention of corona virus infection? *Aging*
447 **12**, 6511–6517 (2020).
- 448 13. Rocs, O. E. OpenEye Scientific Software, Inc., Santa Fe, NM, USA. (2008).
- 449 14. Hawkins, P. C. D., Skillman, A. G. & Nicholls, A. Comparison of shape-matching and
450 docking as virtual screening tools. *J. Med. Chem.* **50**, 74–82 (2007).
- 451 15. Venhorst, J., Núñez, S., Terpstra, J. W. & Kruse, C. G. Assessment of scaffold hopping
452 efficiency by use of molecular interaction fingerprints. *J. Med. Chem.* **51**, 3222–3229
453 (2008).
- 454 16. Sheridan, R. P., McGaughey, G. B. & Cornell, W. D. Multiple protein structures and
455 multiple ligands: effects on the apparent goodness of virtual screening results. *J. Comput.*
456 *Aided Mol. Des.* **22**, 257–265 (2008).
- 457 17. Rush, T. S., 3rd, Grant, J. A., Mosyak, L. & Nicholls, A. A shape-based 3-D scaffold
458 hopping method and its application to a bacterial protein-protein interaction. *J. Med. Chem.*
459 **48**, 1489–1495 (2005).

- 460 18. Haque, I. S. & Pande, V. S. PAPER--accelerating parallel evaluations of ROCS. *J. Comput.*
461 *Chem.* **31**, 117–132 (2010).
- 462 19. FastROCS. OpenEye Scientific Software, Inc., Santa Fe, NM, USA. (2011).
- 463 20. Wójcikowski, M., Kukielka, M., Stepniewska-Dziubinska, M. M. & Siedlecki, P.
464 Development of a protein-ligand extended connectivity (PLEC) fingerprint and its
465 application for binding affinity predictions. *Bioinformatics* **35**, 1334–1341 (2019).
- 466 21. Ballester, P. J. & Richards, W. G. Ultrafast shape recognition to search compound databases
467 for similar molecular shapes. *J. Comput. Chem.* **28**, 1711–1723 (2007).
- 468 22. Armstrong, M. S. *et al.* ElectroShape: fast molecular similarity calculations incorporating
469 shape, chirality and electrostatics. *J. Comput. Aided Mol. Des.* **24**, 789–801 (2010).
- 470 23. Axen, S. D. *et al.* A Simple Representation of Three-Dimensional Molecular Structure. *J.*
471 *Med. Chem.* **60**, 7393–7409 (2017).
- 472 24. Wang, S., Witek, J., Landrum, G. A. & Riniker, S. Improving Conformer Generation for
473 Small Rings and Macrocycles Based on Distance Geometry and Experimental Torsional-
474 Angle Preferences. *J. Chem. Inf. Model.* **60**, 2044–2058 (2020).
- 475 25. Friedrich, N.-O. *et al.* High-Quality Dataset of Protein-Bound Ligand Conformations and
476 Its Application to Benchmarking Conformer Ensemble Generators. *J. Chem. Inf. Model.* **57**,
477 529–539 (2017).
- 478 26. Friedrich, N.-O. *et al.* Benchmarking Commercial Conformer Ensemble Generators. *J.*
479 *Chem. Inf. Model.* **57**, 2719–2728 (2017).
- 480 27. Wójcikowski, M., Zielenkiewicz, P. & Siedlecki, P. Open Drug Discovery Toolkit (ODDT):
481 a new open-source player in the drug discovery field. *J. Cheminform.* **7**, 26 (2015).
- 482 28. Gladysz, R. *et al.* Spectrophores as one-dimensional descriptors calculated from three-

- 483 dimensional atomic properties: applications ranging from scaffold hopping to multi-target
484 virtual screening. *J. Cheminform.* **10**, 9 (2018).
- 485 29. Wang, Y. *et al.* TF3P: Three-Dimensional Force Fields Fingerprint Learned by Deep
486 Capsular Network. *J. Chem. Inf. Model.* **60**, 2754–2765 (2020).
- 487 30. ClinicalTrials.gov. <http://ClinicalTrials.gov>.
- 488 31. Chen, X. & Geiger, J. D. Janus sword actions of chloroquine and hydroxychloroquine
489 against COVID-19. *Cell. Signal.* **73**, 109706 (2020).
- 490 32. Frediansyah, A., Nainu, F., Dhama, K., Mudatsir, M. & Harapan, H. Remdesivir and its
491 antiviral activity against COVID-19: A systematic review. *Clin Epidemiol Glob Health*
492 (2020) doi:10.1016/j.cegh.2020.07.011.
- 493 33. Agrawal, U., Raju, R. & Udhwadia, Z. F. Favipiravir: A new and emerging antiviral option
494 in COVID-19. *Armed Forces Med. J. India* **76**, 370–376 (2020).
- 495 34. Halgren, T. A. Merck molecular force field. I. Basis, form, scope, parameterization, and
496 performance of MMFF94. *Journal of Computational Chemistry* vol. 17 490–519 (1996).
- 497 35. MongoDB Atlas Database. <https://www.mongodb.com>.
- 498 36. Cortés-Cabrera, A., Morris, G. M., Finn, P. W., Morreale, A. & Gago, F. Comparison of
499 ultra-fast 2D and 3D ligand and target descriptors for side effect prediction and network
500 analysis in polypharmacology. *British Journal of Pharmacology* vol. 170 557–567 (2013).
- 501 37. Bonanno, E. & Ebejer, J.-P. Applying Machine Learning to Ultrafast Shape Recognition in
502 Ligand-Based Virtual Screening. *Frontiers in Pharmacology* vol. 10 (2020).
- 503 38. <http://zinc15.docking.org/>. <http://zinc15.docking.org/>.
- 504 39. REAL Database - Enamine. [https://enamine.net/library-synthesis/real-compounds/real-](https://enamine.net/library-synthesis/real-compounds/real-database)
505 [database](https://enamine.net/library-synthesis/real-compounds/real-database).

- 506 40. Optibrium. Optibrium - StarDrop: Nova - A new generation of possibilities.
507 <https://www.optibrium.com/stardrop/stardrop-nova.php>.
- 508 41. Gohda, K., Mori, I., Ohta, D. & Kikuchi, T. 10.1023/A:1008193217627. *Journal of*
509 *Computer-Aided Molecular Design* vol. 14 265–275 (2000).
- 510 42. Mackerell, A. D., Jr. Empirical force fields for biological macromolecules: overview and
511 issues. *J. Comput. Chem.* **25**, 1584–1604 (2004).
- 512 43. Hasegawa, K., Arakawa, M. & Funatsu, K. Rational choice of bioactive conformations
513 through use of conformation analysis and 3-way partial least squares modeling.
514 *Chemometrics Intellig. Lab. Syst.* **50**, 253–261 (2000).
- 515 44. Acharya, C., Coop, A., Polli, J. E. & Mackerell, A. D., Jr. Recent advances in ligand-based
516 drug design: relevance and utility of the conformationally sampled pharmacophore
517 approach. *Curr. Comput. Aided Drug Des.* **7**, 10–22 (2011).
- 518 45. Ullrich, S. & Nitsche, C. The SARS-CoV-2 main protease as drug target. *Bioorganic &*
519 *Medicinal Chemistry Letters* vol. 30 127377 (2020).
- 520 46. Elfiky, A. A. SARS-CoV-2 RNA dependent RNA polymerase (RdRp) targeting: an
521 perspective. *J. Biomol. Struct. Dyn.* 1–9 (2020).
- 522 47. Li, W. *et al.* Angiotensin-converting enzyme 2 is a functional receptor for the SARS
523 coronavirus. *Nature* vol. 426 450–454 (2003).
- 524 48. Vincent, M. J. *et al.* Chloroquine is a potent inhibitor of SARS coronavirus infection and
525 spread. *Viol. J.* **2**, 69 (2005).
- 526 49. Website. *github.com* - *Quantori repository* <https://github.com/quantori/MultiRef3D>.
- 527 50. Targeted Libraries. <https://enamine.net/hit-finding/focused-libraries/>.
- 528

Figures

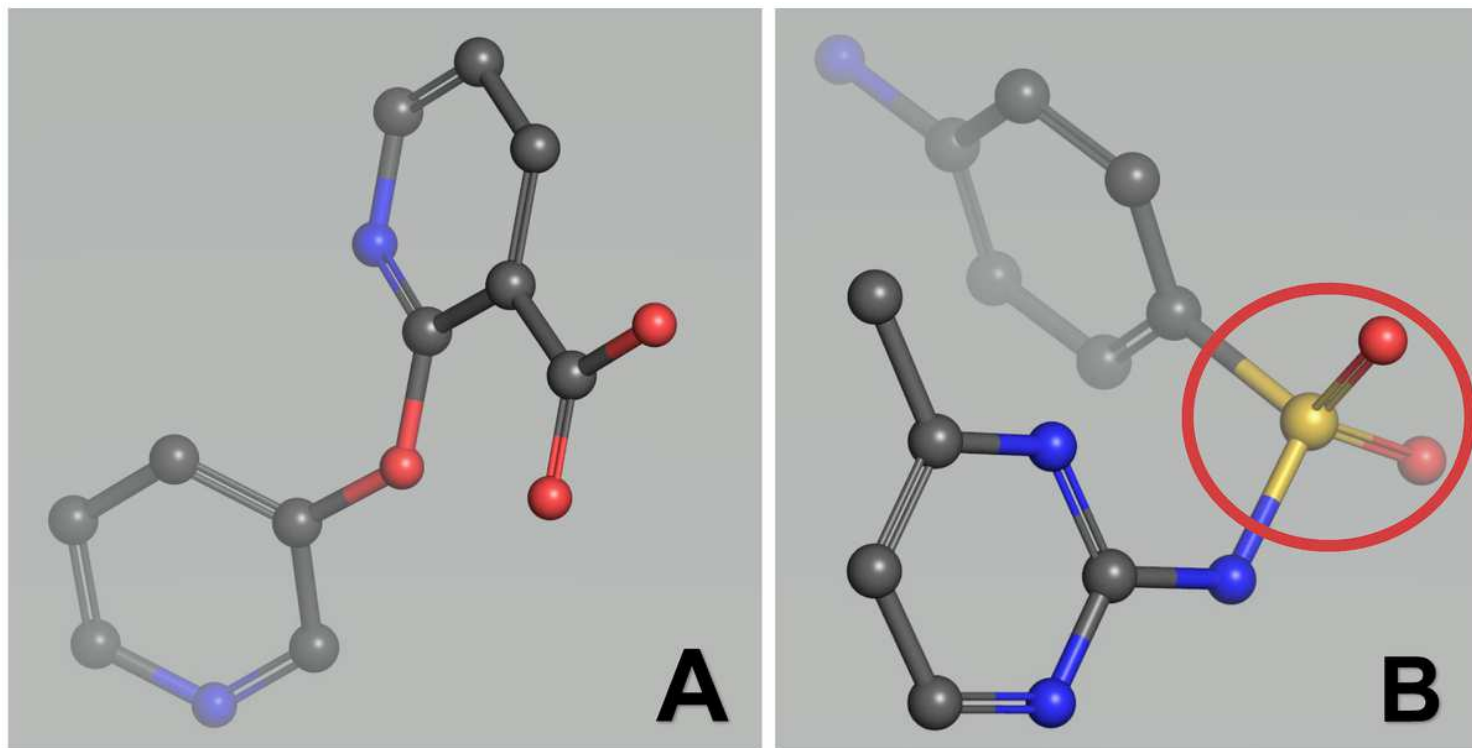


Figure 1

The compounds presented in panels A and B from the antiviral Enamine virtual sub-library collection that were found to maximize conformer overlap scores with the six reference compounds. In addition to that sulphonyl bridge in panel B (circled in red) is a signature of the classic antiviral compounds (e.g. well-known drug sulfapyridine), as well as the ether bond. The bridge allows for 3D flexibility for the molecule to change conformation and bind to multiple targets.

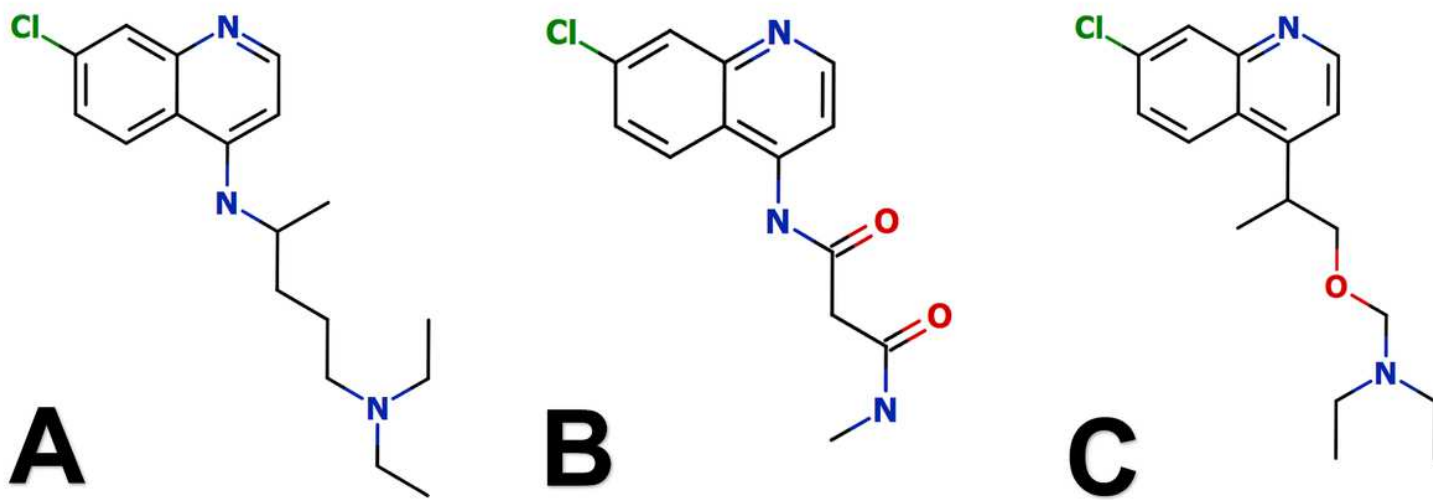


Figure 2

The original chloroquine is presented in panel A, while the chloroquine analogs optimized in the modify-score-select algorithm are presented in panels B and C.